

ETH Zürich

Semester Thesis

**Measurement of Correlation Functions  
with a High Bandwidth FPGA**

**Christian Kern**

Mai 2013

Supervision

**Yves Salathé**

**Jonas Mlynek**

**Prof. Dr. Andreas Wallraff**

This report describes the implementation of first and second order autocorrelation function algorithms with a high speed analog-to-digital converter and a field-programmable gate array in circuit quantum electrodynamics. Results suggest that filtering and first order measurements work properly, however the second order correlation remains to be tested further.

## Contents

<b>1</b>	<b>Introduction</b>	<b>3</b>
1.1	Correlation Functions . . . . .	3
1.2	Setup . . . . .	4
1.3	Previous results . . . . .	4
1.4	Hardware . . . . .	5
1.5	Firmware and Software . . . . .	6
<b>2</b>	<b>Code modifications and extensions</b>	<b>6</b>
2.1	Moving Average Filter - Boxcar . . . . .	7
2.2	Segments and AutoSignalMath . . . . .	9
<b>3</b>	<b>Measurements and Results</b>	<b>10</b>
3.1	First Test Measurements . . . . .	10
3.2	Sample . . . . .	12
3.3	Coherent and thermal sources . . . . .	12
<b>4</b>	<b>Conclusions</b>	<b>15</b>

# 1 Introduction

In circuit quantum electrodynamics (cQED) it is interesting to measure correlation functions which are an important tool to study quantum mechanical effects as for instance the Hong–Ou–Mandel effect [5] and thereby help to validate theoretical predictions.

## 1.1 Correlation Functions

One example for the use of correlation functions is the measurement of photon antibunching in quantum mechanical two-state systems, demonstrating their quantum mechanical nature. Consider a two state system as a perfect single-photon emitter. During the transition  $|1\rangle \rightarrow |0\rangle$  a photon is emitted. Before another photon can be emitted the system has to be excited again. This results in the fact that the time difference between the emission of two photons can't be arbitrarily small, giving a dip at  $\tau = 0$ , which is called antibunching [4].

The first order autocorrelation function is defined as [6]

$$G^{(1)}(\tau) = \langle \hat{a}^\dagger \hat{a}(\tau) \rangle$$

where  $\hat{a}^\dagger$  and  $\hat{a}$  are the creation and annihilation operators of the two-state system. However we are also measuring noise and therefore are not able to measure  $G^{(1)}$  directly but

$$\Gamma^{(1)}(\tau) = \langle \hat{S}^\dagger \hat{S}(\tau) \rangle$$

Now if we switch off the signal and just measure the noise we get the following expression for the correlation function

$$H^{(1)}(\tau) = g_e \langle \hat{h} \hat{h}^\dagger(\tau) \rangle$$

Careful considerations result in a formula for the proper correlation function

$$gG^{(1)}(\tau) = \Gamma^{(1)}(\tau) - H^{(1)}(\tau)$$

where  $g$  is the amplifier gain.

Summarizing:

$G^{(1)}(\tau)$ : First Order Single Channel Autocorrelation

$\Gamma^{(1)}(\tau)$ : Measured First Order Single Channel Autocorrelation

$H^{(1)}(\tau)$ : Noise First Order Single Channel Autocorrelation

The second order autocorrelation function is defined as

$$G^{(2)}(\tau) = \langle \hat{a}^\dagger \hat{a}^\dagger(\tau) \hat{a}(\tau) \hat{a} \rangle$$

Following a similar derivation we will arrive at

$$g^2 G^{(2)}(\tau) = \Gamma^{(2)}(\tau) - H^{(2)}(\tau) - 2gG^{(1)}(0)H^{(1)}(0) - gG^{(1)}(-\tau)H^{(1)}(\tau) - gG^{(1)}(\tau)H^{(1)}(-\tau)$$

We use the well known convolution theorem (with a factor depending on convention)

$$F(f * g) = F(f) \cdot F(g), \quad f, g \in L^1(\mathbb{R})$$

Let  $I$  and  $Q$  denote the quadratures of the signal. This enables us to determine the correlation functions in our setup in the following way

$$G1 : \text{IFFT} (\langle \text{FFT} (I + iQ) \cdot \text{FFT} (I + iQ)^* \rangle)$$

$$G2 : \text{IFFT} (\langle \text{FFT} ((I + iQ) \cdot (I + iQ)^*) \cdot \text{FFT} ((I + iQ) \cdot (I + iQ)^*)^* \rangle)$$

The fast Fourier transform (FFT) is a very efficient algorithm for computing the discrete Fourier transform. It allows the rapid computation of convolutions.

## 1.2 Setup

A typical setup used for cQED experiments as it was also used for our measurements is shown in Figure 1 . On the left the generation of a probe microwave tone (in our setup at  $\sim 7$  GHz) is shown. Therefore a low frequency ( $\leq 500$  MHz) signal from an arbitrary waveform generator (AWG) is upconverted using a microwave generator. Both can be controlled by a PC, usually using LabView. Normally the AWG patterns are created with Mathematica. The probe tone is then sent to the sample inside the cryo. The outgoing signal is again down converted and digitized using a high bandwidth analog-to-digital converter. The digitized signal is processed using a field-programmable gate array (FPGA) including for example a fast Fourier transform and the result transferred to a PC. Up and down conversion are used since it is much simpler to handle signals at frequencies below 500 MHz, for example when it comes to digitizing.

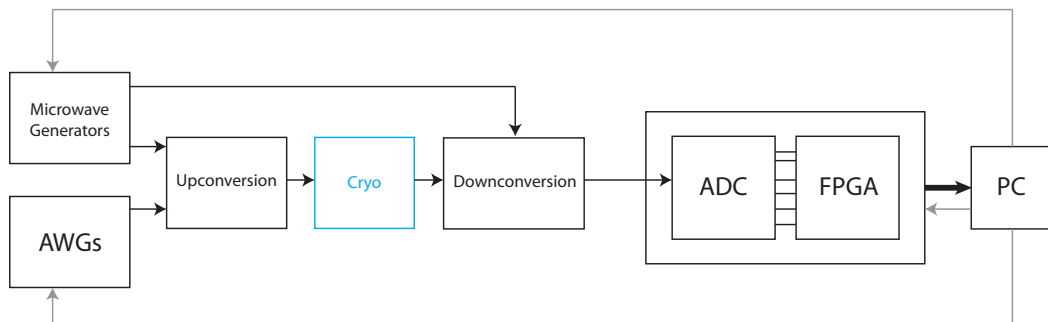


Figure 1: Schematic of the setup used for our measurements, description in the text

## 1.3 Previous results

Correlation functions are used to observe antibunching in circuit quantum electrodynamics, showing the quantum mechanical character of a single photon emitter [7] . It is also interesting to look at a thermal source, filtered by a resonator, or a coherent source [8] . For a coherent source the second order correlation function is simply a constant. For a thermal source one observes photon bunching.

## 1.4 Hardware

As mentioned above, the digitized signals are processed using a field-programmable gate array (FPGA). An easy way to fancy an FPGA is to think of a chip providing logic functions that can be programmed. It is a tool to implement quasi arbitrary integrated circuits that can be reconfigured. FPGAs process information parallel. By contrast a central processing unit (CPU) works in principle sequentially. An FPGA usually pays off compared to microprocessors when it comes to large amounts of data at high speeds.

In our group most experiments are done using hardware (featuring a Virtex 4 FPGA) with a bandwidth of  $\sim 50$  MHz. For the present thesis new hardware, introduced in previous work [1], was used with the main advantage of a higher bandwidth. It features a Xilinx ML605 evaluation board, shown in Figure 2 , with a Virtex 6 FPGA and a 4DSP FMC110 daughter card (FPGA Mezzanine Card - FMC), shown in Figure 3, with two TI 1 GS/s ADCs. The Virtex 6 has more logic cells, slices et cetera compared to the Virtex 4 and hence offers more possibilities. A more detailed depiction is given in [1].

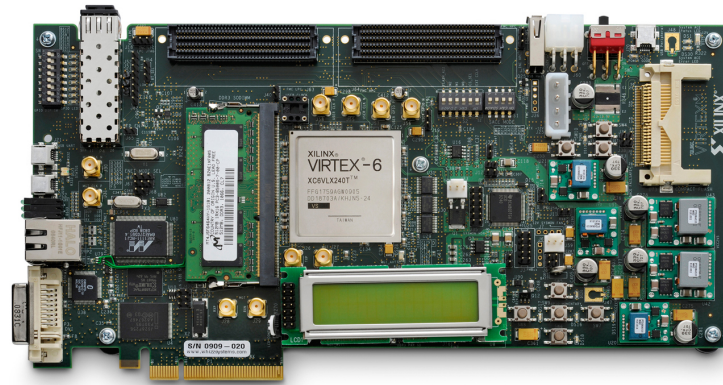


Figure 2: The Xilinx ML605 evaluation board, taken from [2]

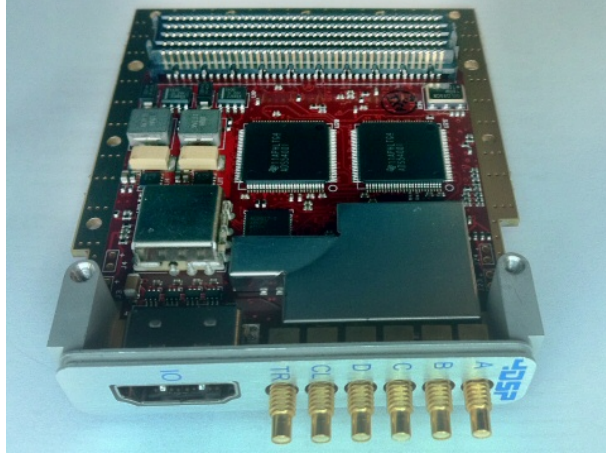


Figure 3: The 4DSP FMC110 Analog-to-Digital converter board, taken from [3]

### 1.5 Firmware and Software

The programming of the FPGA is done in Simulink and VHDL. The present thesis deals primarily with extensions to the code written by Yves Salathé (Figure 4).

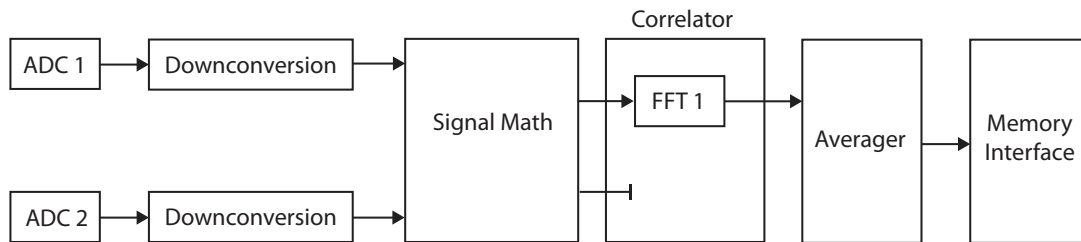


Figure 4: Schematic of the Simulink code.

First of all the digitized signals from two ADCs are downconverted to a fixed intermediate frequency of 250 MHz. SignalMath is a block which enables the user to choose the input to the FFT by writing a register of the FPGA, normally via LabView. The Fourier transformed signal is then averaged over many shots in order to improve the SNR.

LabView software is used to conduct the measurements, control AWGs and microwave generators and check the obtained data. Also a C++ library was written in previous work [1] to communicate with the FPGA, write registers and read and write the memory.

## 2 Code modifications and extensions

The main task now was to extend the code to second order autocorrelation functions. So far we were limited to timetraces, first-order autocorrelation functions and power spectral

densities. Figure 5 shows the schematic of the Simulink code after the modifications.

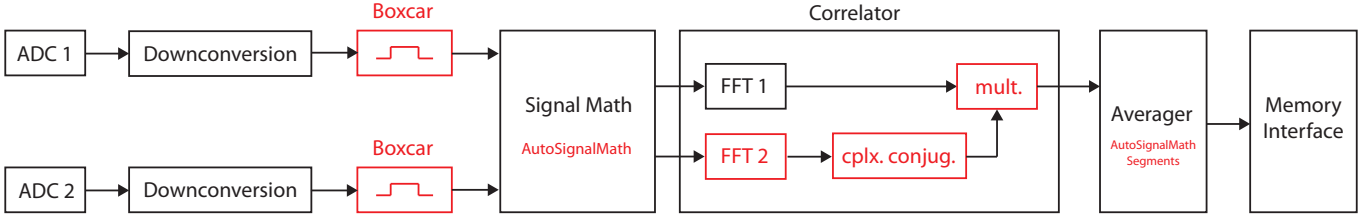


Figure 5: Schematic of the modified Simulink code.

In principle the code is just a realisation of the equation given in section 1.1 . A second FFT was added. This is in principle not necessary for autocorrelation measurements but already paves the way for future crosscorrelation measurements.

AutoSignalMath which is described below is an extension to SignalMath which automatically changes the input of the FFT. This makes it possible to measure the correlation functions for noise and the signal almost simultaneously.

Since noise, especially DC noise, has an effect on the correlation functions, filtering becomes necessary. In case of G2 we are performing a nonlinear operation ahead of the FFT. This makes it impossible to perform the filtering afterwards since these operations do not commute.

## 2.1 Moving Average Filter - Boxcar

We realised the most probable simplest filter one can think of, an eight point moving average filter with constant coefficients (boxcar filter). Since an eight point boxcar has a node at  $-250$  MHz the DC Noise which is at  $-250$  MHz after the downconversion gets suppressed. The filter function reads

$$\tilde{s}_i = \frac{1}{8} \sum_{j=0}^7 s_j$$

with a frequency response given by [9]

$$H(f) = \frac{\sin(8\pi f)}{8 \sin(\pi f)}$$

The Simulink code shown is implemented with a clock frequency of 125 MHz. This makes it necessary to process eight samples in parallel. Therefore already a simple boxcar gets quite complicated.

Figure 6 shows a simplified version of the Simulink code implemented.

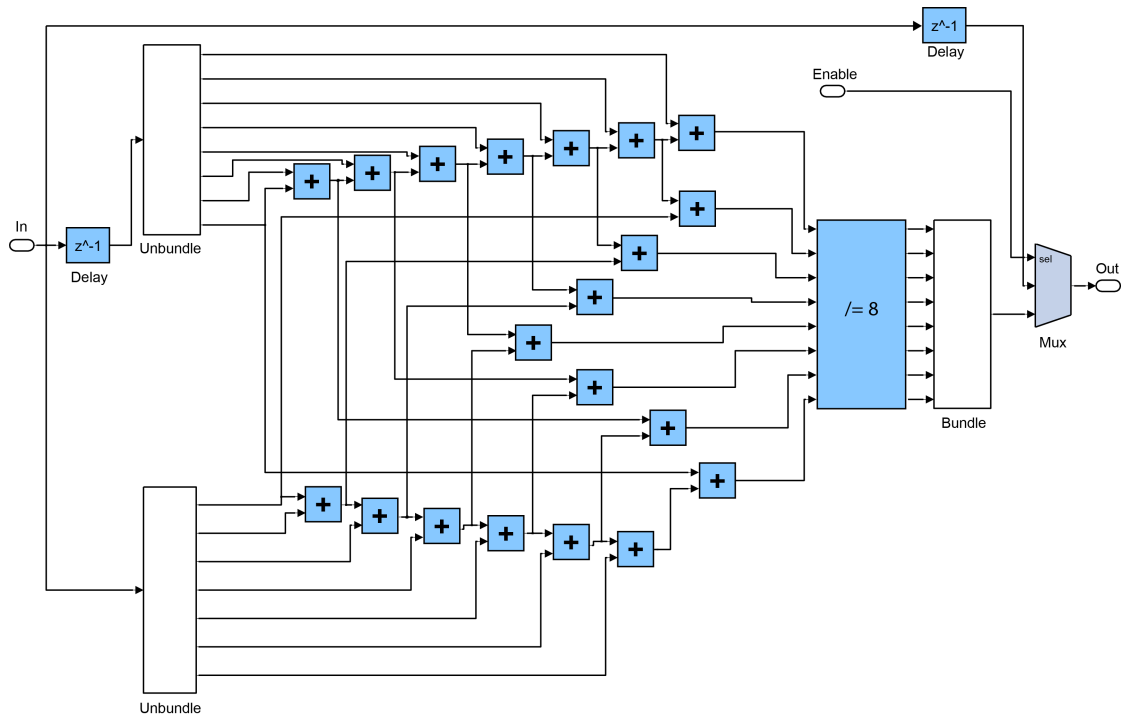


Figure 6: Simplified Simulink code for the boxcar filter, first the eight parallel samples are unbundled, then added successively, keeping the number of adders small. The result is divided by eight. In the end the filtered samples are again bundled. The whole filter can be deactivated using a register and a multiplexer.

The frequency response was determined using almost white noise from an AWG and comparing the spectra of the filtered with the unfiltered noise. It is shown in Figure 7 .



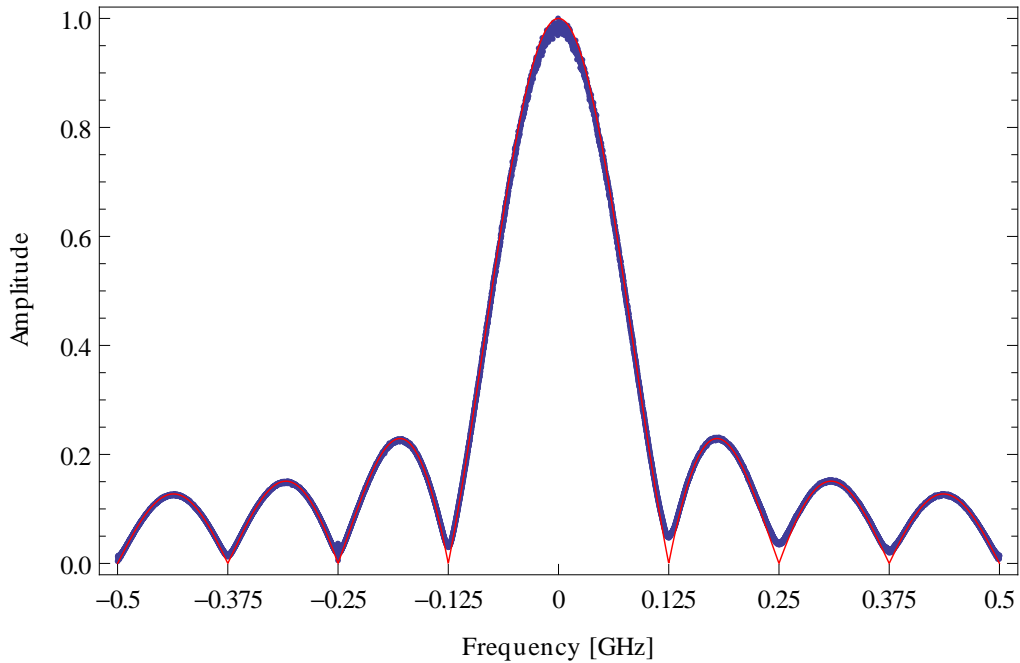


Figure 7: Frequency response of the boxcar filter. Measured quantities are shown in blue, theory in red

## 2.2 Segments and AutoSignalMath

AutoSignalMath is a part of the FPGA firmware written previously for the Virtex 4 by Christian Lang using Simulink and VHDL. It cycles the input of the FFT through a specified list from pattern to pattern. Via software the user can choose from different predefined pattern lists. This makes it possible to measure first and second order autocorrelation functions for noise and signal which are averaged separately resulting in four different segments almost simultaneously. To be precise first the input is chosen so that first order functions can be measured. It stays the same for two measurements. Then the same is done for the second order functions.

This makes the calculation of the proper autocorrelation function, as described here, much simpler (we need less averages) since the noise changes over time.

Given that the code was already existing for the Virtex 4 it was simple to implement it for the Virtex 6.

### 3 Measurements and Results

The second part of the work focused on test measurements. After a few simple tests it was the aim to use the system in a real measurement setup where the high bandwidth is useful.

#### 3.1 First Test Measurements

In order to check proper functioning of the modifications implemented a very simple setup, shown in Figure 8 was used.

An Arbitrary Waveform Generator (AWG) was directly connected to the ADC input of the FMC110 card, additionally providing a trigger. A 10 MHz Rubidium Frequency Standard was used as a clock. For different test patterns generated with Mathematica and played with the AWG time traces,  $G_1$  and  $G_2$  were measured.

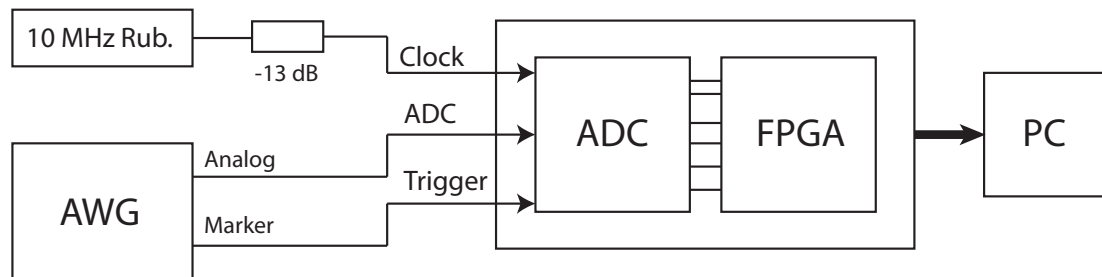


Figure 8: Schematic of the setup used for the first test measurements

Figure 9 shows one test pattern and the corresponding  $G_1$  and  $G_2$  as well as the theoretical determined functions.

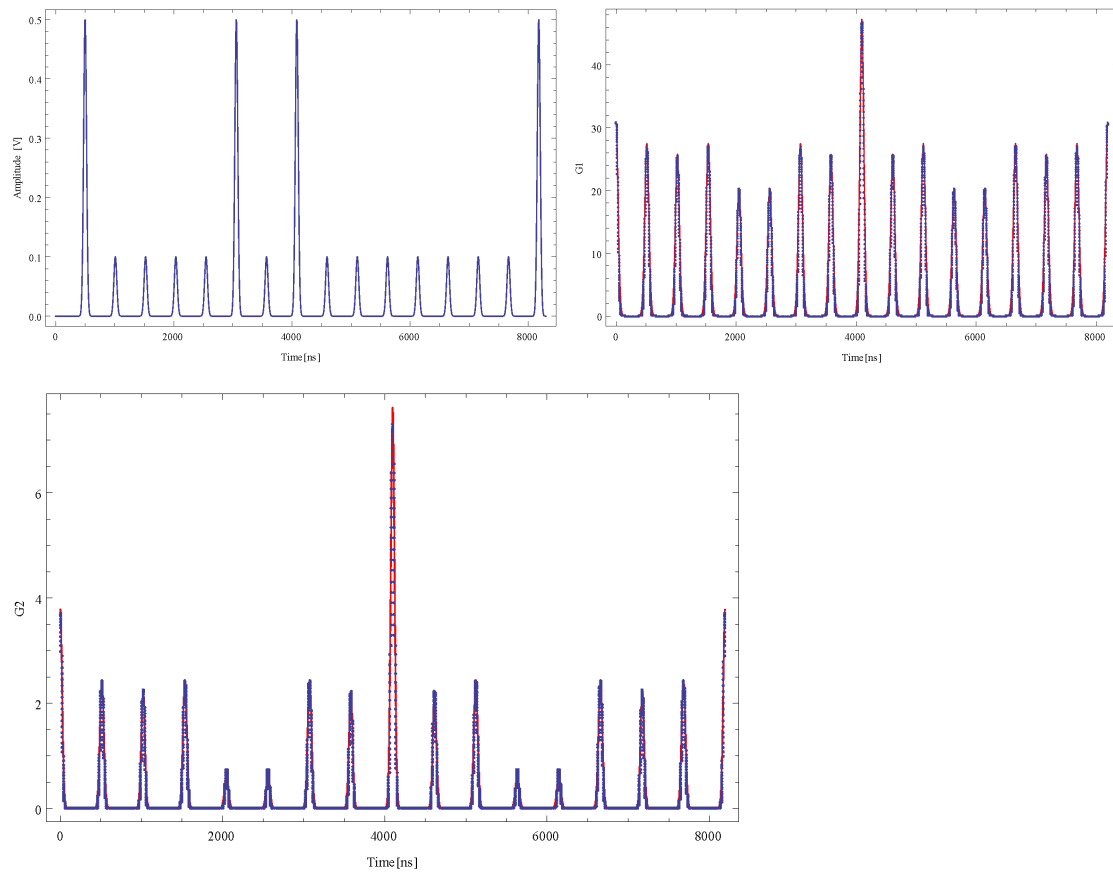


Figure 9: From top left: The envelope of the 250 MHz test pattern used, G1 and G2. Measured quantities are shown in blue, theory in red

The measurements are in good agreement with the results expected, as also visible from Figure 9.

## 3.2 Sample

Measurements were done with a three-qubit sample shown in Figure 10 designed and fabricated by Jonas Mlynek.

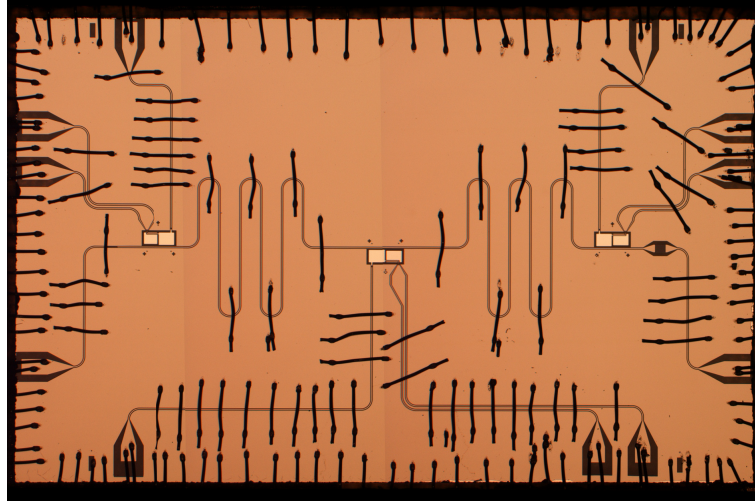


Figure 10: The sample used for our measurements after bonding. Optical microscope image.

The main parameters are:

- $\frac{1}{\kappa} \approx 20$  ns
- $\frac{2\pi}{g} \approx 200$  ns
- $\nu_0 \approx 7$  GHz
- $T_2 \approx 400$  ns

The sample fulfils the so called bad cavity limit meaning  $\kappa \gg g \gg \gamma$ . The parameters suggest the use of high bandwidth measurement techniques.

## 3.3 Coherent and thermal sources

We chose to look at thermal noise and a coherent source. For the coherent source we simply used a microwave generator. For thermal noise we used the white noise output of a Tektronix AWG with a bandwidth of  $\sim 500$  MHz. After upconversion this gives almost white noise from 6.5 GHz to 7.5 GHz. A DC-offset for calibration is applied at the mixer to avoid LO leakage. Both signals were sent through the resonator. Figure 11 shows a schematic of the setup.

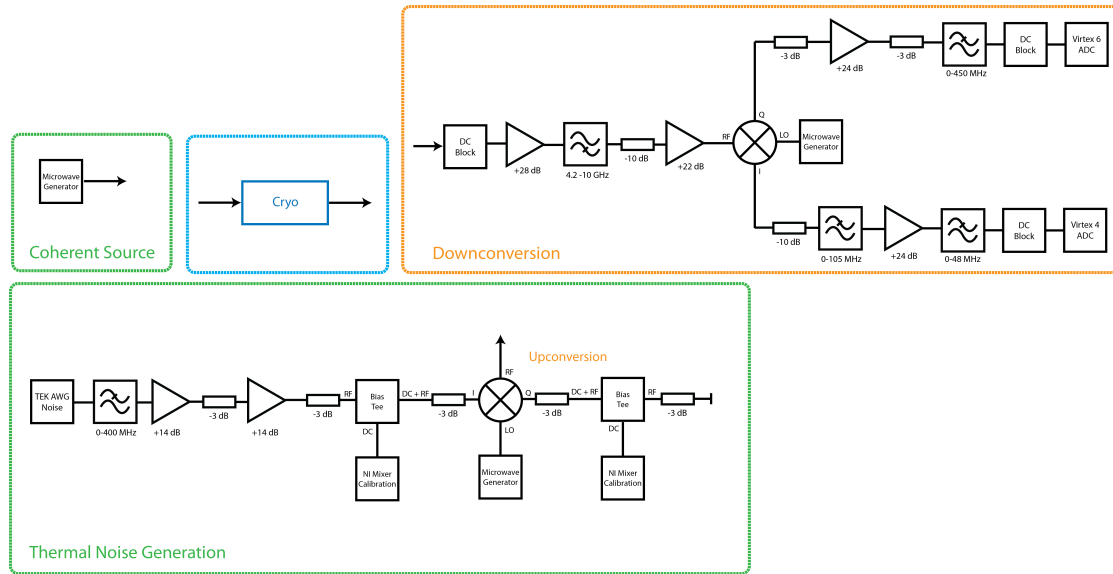


Figure 11: The Setup used for measurements of thermal noise and a coherent source. On the left side the noise generation is shown. On the right side one can see the downconversion, amplification and filtering as well as the ADCs

The power spectral density is just the Fourier transform of the first order autocorrelation function. It is shown for thermal noise filtered by the resonator in Figure 12 . The same with one qubit tuned on resonance is shown in Figure 13 .

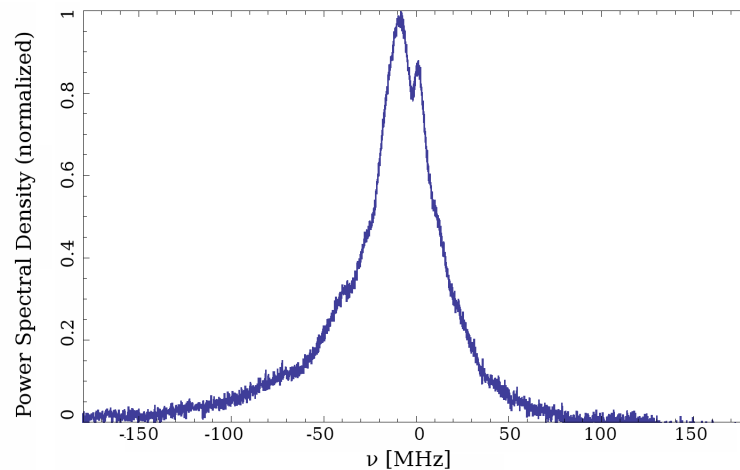


Figure 12: The power spectral density of the thermal noise through the resonator. The non-constant amplifier gain is visible. The central dip is so far not fully understood.

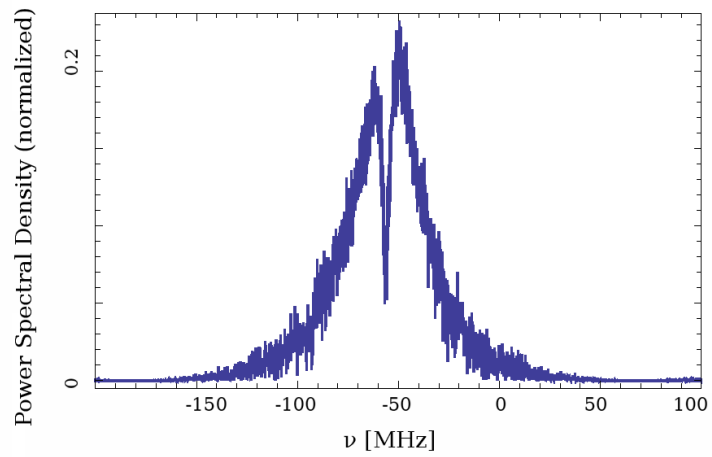


Figure 13: The power spectral density of the thermal noise through the resonator with on of the qubits tuned on resonance. A simple classical model is a driven damped harmonic oscillator coupled to another damped harmonic oscillator.

Figure 14 shows the corrected second order autocorrelation function and a comparison with theory. The triangular shape looks somehow suspicious indicating that there is still something going wrong.

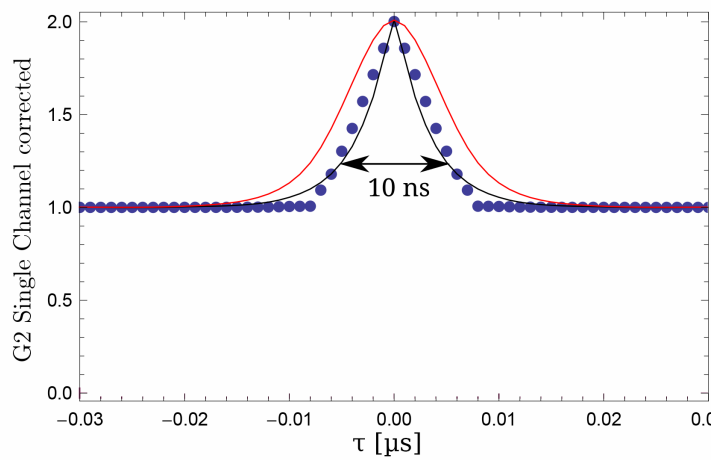


Figure 14: The corrected second order autocorrelation function. Black: Simulation, Red: Simulation accounting for finite sampling rate, Blue: Measured Values

## 4 Conclusions

An existing data acquisition system for measurements in circuit quantum electrodynamics was extended to measure autocorrelation functions. It was tested with overall positive results however further analysis for the second order functions is necessary. Therefore the next steps will involve more tests and evaluation.

It will be an interesting task to extend the work presented here to higher order and crosscorrelation functions.

## Acknowledgements

First of all I want to thank Prof. Andreas Wallraff for the opportunity to work in his lab. I would like to thank Yves Salathe who supervised the technical part and Jonas Mlynek who supervised the experimental part. I'd also like to thank Christian Lang for his help.

## References

- [1] Yves Salathe, Master Thesis  
*Towards Gigahertz Bandwidth Digital Signal Processing in Circuit Quantum Electrodynamics*, October 2011, ETH Zürich
- [2] Xilinx ML605 evaluation board  
<http://press.xilinx.com/index.php?s=20291&mode=gallery&cat=2764>
- [3] 4DSP, FMC110  
<http://www.4dsp.com/FMC110.php>
- [4] Wikipedia, the free encyclopedia, visited April 2013.  
[http://de.wikipedia.org/wiki/Photon\\_Antibunching](http://de.wikipedia.org/wiki/Photon_Antibunching)
- [5] C. Lang, C. Eichler, L. Steffen, J. M. Fink, M. J. Woolley, A. Blais and A. Wallraff  
*Correlations, indistinguishability and entanglement in Hong–Ou–Mandel experiments at microwave frequencies*, Nature Physics (2013) (2010)
- [6] Marcus P. da Silva, Deniz Bozyigit, Andreas Wallraff and Alexandre Blais  
*Schemes for the observation of photon correlation functions in circuit QED with linear detectors*, Phys. Rev. A 82, 043804 (2010)
- [7] D. Bozyigit, C. Lang, L. Steffen, J. M. Fink, C. Eichler, M. Baur, R. Bianchetti, P. J. Leek, S. Filipp, M. P. da Silva, A. Blais and A. Wallraff  
*Antibunching of microwave-frequency photons observed in correlation measurements using linear detectors*, Nature Physics 7, 154–158 (2011)
- [8] C. Lang, D. Bozyigit, C. Eichler, L. Steffen, J. M. Fink, A. A. Abdumalikov, Jr., M. Baur, S. Filipp, M. P. da Silva, A. Blais, and A. Wallraff  
*Observation of Resonant Photon Blockade at Microwave Frequencies Using Correlation Function Measurements*, Phys. Rev. Lett. 106, 243601 (2011)
- [9] Steven W. Smith *The Scientist and Engineer’s Guide to Digital Signal Processing*, California Technical Publishing, ISBN 0-9660176-7-6